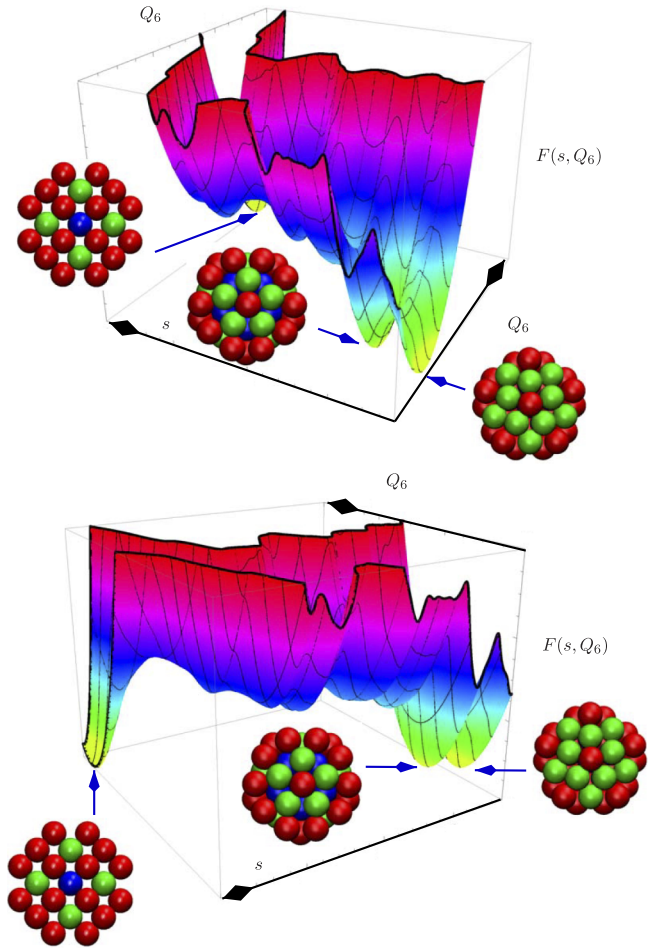

FIG. 5. Two views of the free energy surface obtained from $-k_BT \ln P(s)$ $P(Q_6|s)$ for constraint distance 0.4 and $k_BT/\epsilon = 0.12$. The positions of three low-lying minima are marked.[159]

surface packings is apparent for the s coordinate. However, when a one-dimensional projection onto Q_6 is employed, the two minima (and the barrier region) are simply averaged over.

The results for $F(s)$ in Figure 4 exhibit some systematic trends. For $d = 0.4$, the shortest constraint distance, there is little temperature dependence. In contrast, for $d = 1.0$, $F(s)$ shifts systematically to a narrower range as the temperature increases, but the positions of local maxima and minima are preserved. The effects of changing constraint distance and temperature on $F(Q_6)$ are similar (Figure 6), but the plots are dominated by two deep free energy minima corresponding to Q_6 values around 0.14 and 0.55 for icosahedral and fcc structure, respectively. These minima are consistent with the profiles obtained in previous work using parallel tempering and adaptively biased Monte Carlo.[159] Precise agreement is not expected, since the full configuration space is accessible in the latter calculations. For example, a shallower minimum corresponding to decahedral packing is then observed around $Q_6 = 2.8$.[159] For the single pathway examined here, such structure does not arise. One further check was performed to verify that $F(s)$ approaches $V(s)$, the potential energy defined by the reference configurations, at low temperature.

Results for one of the path segments connecting two adjacent minima are shown in Figure 7. This section of the path, corresponding to the fifth transition state in Table I,

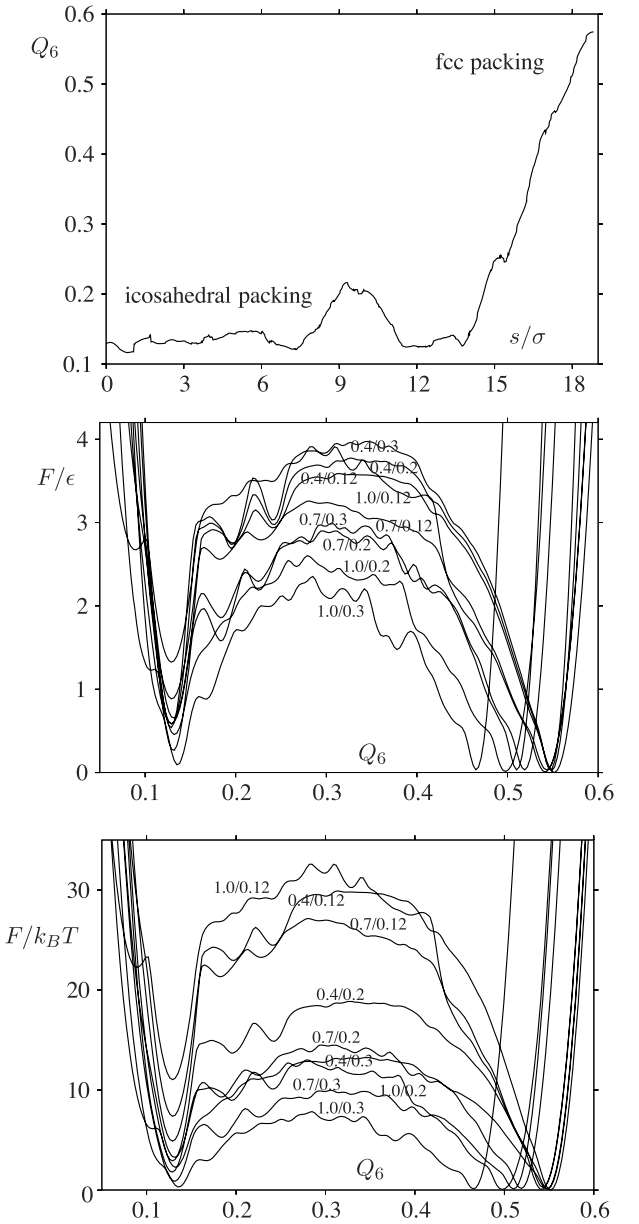

FIG. 6. Top: Q_6 as a function of the configurations characterising an interconversion pathway of LJ_{38}. Middle: free energy F as a function of Q_6 for the same path. The results correspond to constraining distances $d = 0.4$, 0.7, and 1.0 and temperatures $k_BT/\epsilon = 0.12$, 0.2, and 0.3, as marked on the plots. Bottom: as for the middle plot but illustrating $F(Q_6)/k_BT$ for comparison with previous work.

is interesting because it exhibits a bimodal distribution for Q_6 (Figure 7). The minima have Q_6 values of 0.20 and 0.12 and are sufficiently similar in energy to have comparable occupation probabilities for the temperature range considered here. This example is selected to illustrate the agreement between Q_6 distributions calculated in different ways. Results are compared for direct visit statistics for the Q_6 bins using a single block containing all the reference configurations, average values of Q_6 for instantaneous and reference configurations for the s bins weighted by $P(s)$, and a harmonic superposition calculation,[1,54–56] which only uses the Q_6 values for the two minima. The distributions agree very well, particularly at this relatively low temperature, where anharmonic effects are small.